Degenerative Age Changes in White Matter Connectivity Visualized *In Vivo* using Magnetic Resonance Imaging

Christos Davatzikos and Susan M. Resnick[1]

Department of Radiology, Johns Hopkins University School of Medicine and [1]Laboratory of Personality and Cognition, National Institute on Aging, Baltimore, MD, USA

Age effects on the signal characteristics of white matter (WM) were examined via magnetic resonance imaging (MRI). Global and local patterns of WM degeneration were demonstrated using a new image analysis methodology. Significant cross-sectional and longitudinal age effects were found in the WM, primarily in the left hemisphere. Importantly, signal changes, which likely reflect WM demyelination, and changes in water, protein and mineral content of tissue, were unrelated to volumetric changes. Thus, measures of tissue characteristics provide unique and complementary information to widely used measures of brain atrophy. Moreover, signal measurements displayed stronger associations with age and can potentially be more sensitive than volumetric measures as indicators of preclinical disease, because they reflect changes in the underlying tissue composition. To our knowledge, our study is the first documentation of longitudinal age- and region-dependent changes in magnetic resonance signal characteristics of WM fibers, reflecting underlying degenerative effects of aging.

Introduction

Magnetic resonance imaging (MRI) has been used extensively in studies of brain aging, because it provides high resolution *in vivo* images that may aid in the prediction of individuals at risk for memory impairment and Alzheimer's disease (Convit *et al.*, 1997; Jack *et al.*, 2000). Many investigators have performed global or regional volumetric measurements of grey matter (GM), white matter (WM) and cerebrospinal fluid (CSF), characterizing the degree of brain atrophy with normal aging or disease (Coffey *et al.*, 1992; Pfefferbaum *et al.*, 1994; Kaye *et al.*, 1997; Raz *et al.*, 1997; Mueller *et al.*, 1998; Pruessner *et al.*, 2000). Other studies have used the framework of shape transformations (Bookstein *et al.*, 1989; Miller *et al.*, 1993; Davatzikos *et al.*, 1996; Thompson *et al.*, 1997; Freeborough and Fox, 1998a; Davatzikos, 2000) to characterize local variability in brain morphology. Despite the large number of studies that measure brain shape and volume, there is a lack of analogous studies examining how the signal characteristics of different brain tissues are affected by normal or pathological aging. Some investigators have shown that image texture analysis can potentially be a useful tool for image-based diagnosis of Alzheimer's disease (Freeborough and Fox, 1998b; Kovalev *et al.*, 2001), but analyses to date have been performed for the whole brain and have not examined regional variability in signal characteristics. In this paper, we apply a new methodology based on high-dimensional elastic transformation to demonstrate substantial cross-sectional and longitudinal age and regional effects on the signal characteristics of GM and WM. We focus primarily on the signal properties of WM, because they reflect changes in myelination of the underlying connective fibers in the brain and impact inter-regional transmission of information. Our results provide the first *in vivo* evidence of degenerative age changes in WM connectivity, measured by longitudinal changes in MRI signal characteristics in a group of nondemented older adults.

The characterization of signal changes with aging or disease provides important information that is complementary to morphometric studies of regional brain volumes. The deposition of plaques and tangles in Alzheimer's disease is likely directly to influence the signal properties of affected tissue, since it changes the tissue composition. For example, changes in T_2^* proton signal in amyloid plaques have been identified with post-mortem MRI and a high field magnet (Benveniste *et al.*, 1999). In contrast, morphometric studies only indirectly measure these changes via displacements that are observed at adjacent tissue boundaries and that allow for the definition of regions of interest and volumetric measurements (Goldszal *et al.*, 1998; Collins *et al.*, 1999) or for the calculation of shape deformation fields (Bookstein *et al.*, 1989; Miller *et al.*, 1993; Davatzikos *et al.*, 1996; Thompson *et al.*, 1997; Freeborough and Fox, 1998a; Gaser *et al.*, 1999; Ashburner and Friston, 2000; Davatzikos, 2000). However, such shape measurements are limited in many respects. In particular, marked shape changes are likely to occur at relatively late stages of the development of disease, when neuronal death and brain atrophy are observed. Moreover, these indirect shape changes may be small, depending on how close the affected tissue is to tissue boundaries and other features that can be reliably identified in tomographic images. Thus, quantification of global and local changes in tissue composition characteristics, reflected by characteristics of the magnetic resonance signal, may provide additional information. This unique and complementary information may enhance the preclinical detection of memory impairment and Alzheimer's disease.

Materials and Methods

Tissue signal characteristics and brain volumes were measured from 'spoiled grass' (SPGR) volumetric magnetic resonance images (axial acquisition; T_R = 35 ms, T_E = 5 ms, flip angle = 45°, matrix = 256 × 256, field of view = 24 cm, N_{ex} = 1) from 91 older adults, ranging in age from 59.6 to 85.9 years (mean ± SD 70.3 ± 7.0 years) at baseline evaluation. These individuals are participants in the neuroimaging substudy of the Baltimore Longitudinal Study of Aging (BLSA) and have completed at least 5 years of annual neuroimaging evaluations. The sample included 49 men and 42 women. Means ± SD for age were 70.3 ± 6.4 years for men and 70.4 ± 7.7 years for women. Eighty-two participants were Caucasian and nine were African-American; three men and two women were not right handed. Average education in this sample was 16.2 ± 2.7 years, consistent with the average educational level of the BLSA as a whole. In the present report, assessments at baseline (year 1) and years 3 and 5 were analyzed for examination of age differences and changes over 4 years in brain tissue characteristics. Volumetric data for years 1 and 2 are available (Resnick *et al.*, 2000). This study was approved by the local institutional review board and all subjects gave written informed consent.

To quantify the signal characteristics of WM and GM, images were first segmented into GM, WM and CSF using an automated algorithm for tissue classification (Yan and Karp, 1995; Goldszal *et al.*, 1998). We first quantified global signal characteristics by determining the average grey and white matter intensities throughout the whole brain. To eliminate

global signal scaling effects, a contrast ratio (CR) was calculated as the ratio of the difference between white and grey matter intensities to their average value. Moreover, in order to remove the effects of magnetic field inhomogeneities, we applied an iterative inhomogeneity correction algorithm that has been published and tested in the literature (Pham and Prince, 1999). Longitudinal age changes, in contrast, were examined using mixed effects regression analysis as implemented by SAS v. 8.1 under OpenVMS. Age at baseline evaluation, sex and time (baseline, year 3, year 5) were entered as predictors and global contrast for each time point was the dependent measure.

The interpretation of global brain changes is inherently limited due to the high degree of functional specialization throughout the brain. To examine regionally specific effects of age, a voxel-wise regional signal analysis of the magnetic resonance images was performed, focusing on WM signal intensities. Images were first spatially normalized using a three-dimensional elastic warping method (Davatzikos, 1997) that placed the images into stereotaxic coordinate space (Talairach and Tournoux, 1988) and accounted for inter-individual variability in overall brain shape and size. Our elastic transformation was particularly designed to account for enlargement of the ventricles that is prominent in elderly subjects. Magnetic resonance signal characteristics at each WM voxel in the stereotaxic space were then determined. A regional contrast ratio (rCR) was calculated as:

$$2[WM(\mathbf{x}) - GM]/[WM(\mathbf{x}) + GM]$$

where $WM(\mathbf{x})$ is the local WM intensity at a voxel $\mathbf{x}$ and GM is the global average of the GM intensity throughout the whole brain. Values were normalized to the global GM intensity value to adjust for global scanner gain factors. To reduce noise, images were smoothed by averaging WM intensity values within a spherical neighborhood of 10 mm radius.

The significance of age differences and longitudinal changes in WM-rCR at each voxel location was examined via voxel-wise *t*-tests and paired *t*-tests, respectively. We examined age differences (59–69 versus 70–85 years at baseline) and longitudinal change over 4 years for the entire sample, as well as separately for men and women.

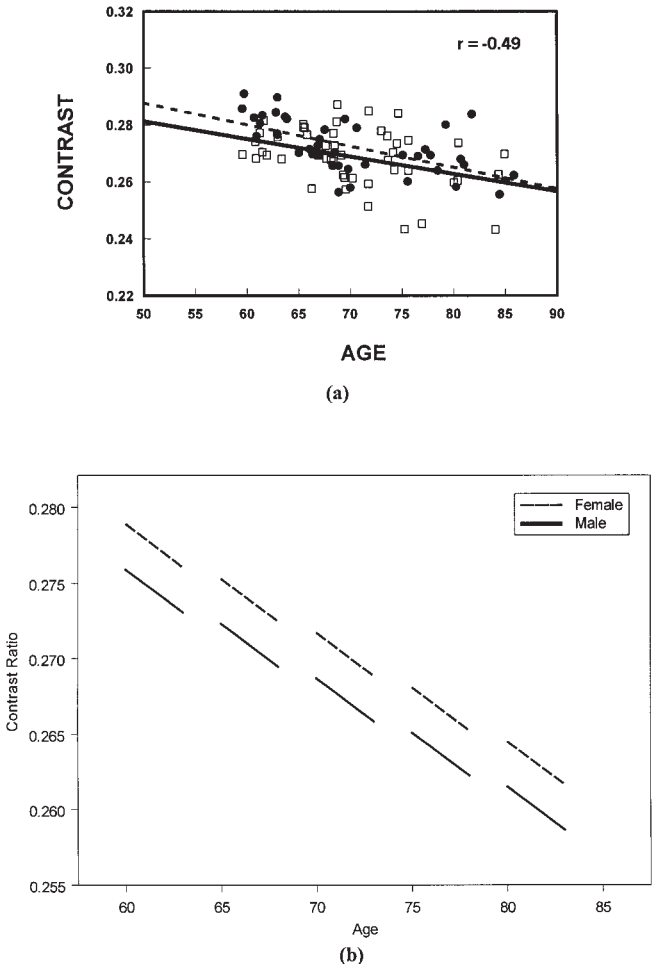

Figure 1. (*a*) Correlation between global measures of white/grey matter signal contrast and age at baseline evaluation (men – open squares, solid line; women – filled circle, dashed line). (*b*) Age differences and longitudinal change in white/grey matter contrast. This figure plots the parameter estimates from the mixed effects regression analysis, illustrating age differences and within-individual changes in 5 year age bands. The linear decreases in the magnitude of the CR across age groups show cross-sectional age differences, with older individuals having lower CR. Within-individual longitudinal declines are reflected by the slopes of the lines and show similar rates of change for all age groups.

Results

Figure 1*a* shows the association between age and CR at baseline evaluation, indicating significant cross-sectional declines in CR with age for both men (r = –0.39, $P < 0.01$) and women (r = –0.62, $P < 0.001$). Consistent with the simple correlations, results of the mixed effects regression analysis revealed highly significant cross-sectional effects of age at baseline evaluation [$F(1,91) = 38.3$, $P < 0.0001$]. A highly significant effect of time [$F(1,90) = 23.2$, $P < 0.0001$] indicated longitudinal declines in the CR over the 4 year interval. Figure 1*b* shows a plot of the parameter estimates from the mixed effects regression analysis, illustrating linear differences between age groups and longitudinal changes within each group. There were no significant sex differences or interactions among predictors, indicating similar rates of change for men and women and for younger and older participants. The decrease in CR with age was independent of age-related changes in brain volume, as the correlations between longitudinal change in CR and longitudinal change in brain volumes were near 0 (r = 0.03 for total brain volume, r = –0.03 for WM volume, r = 0.06 for GM volume). This absence of significant associations between longitudinal changes in CR and volumes indicates that tissue contrast measurements provide unique information beyond that of the typically employed volumetric atrophy measurements.

Results from our analysis of the rCR are shown in Figures 2 and 3, for men and women combined. To facilitate visualization of the results, we display the regions with significant age effects on an image that was created by averaging the GM distribution among all subjects after spatial normalization. In generating this average image, the exact same spatial transformations that were applied to the T_1 images were applied to the respective segmented images. Brighter regions of the image are more likely to contain GM. This average map provides a reference for anatomical localization of the observed age effects. Figure 2 shows cross-sectional effects of age examined via voxel-wise *t*-tests and Figure 3 shows longitudinal changes examined via voxel-wise paired *t*-tests. Both cross-sectional and longitudinal analyses revealed pronounced age effects on WM-rCR for frontal, parietal and temporal, but not occipital regions. In general, there was a clear inter-hemispheric difference for both cross-sectional and longitudinal results, with the left hemisphere showing larger age effects on WM-rCR. Inter-hemispheric differences were evident in the frontal and temporal regions, but pronounced age effects occurred bilaterally in the parietal WM. Longitudinal findings were more pronounced than cross-sectional age effects, likely due to the inherent increases in sensitivity for within-subject longitudinal analyses, which reduce inter-individual variability. When men and women were analyzed separately, similar spatial patterns were observed with relatively lower degrees of statistical significance due to the smaller sample sizes.

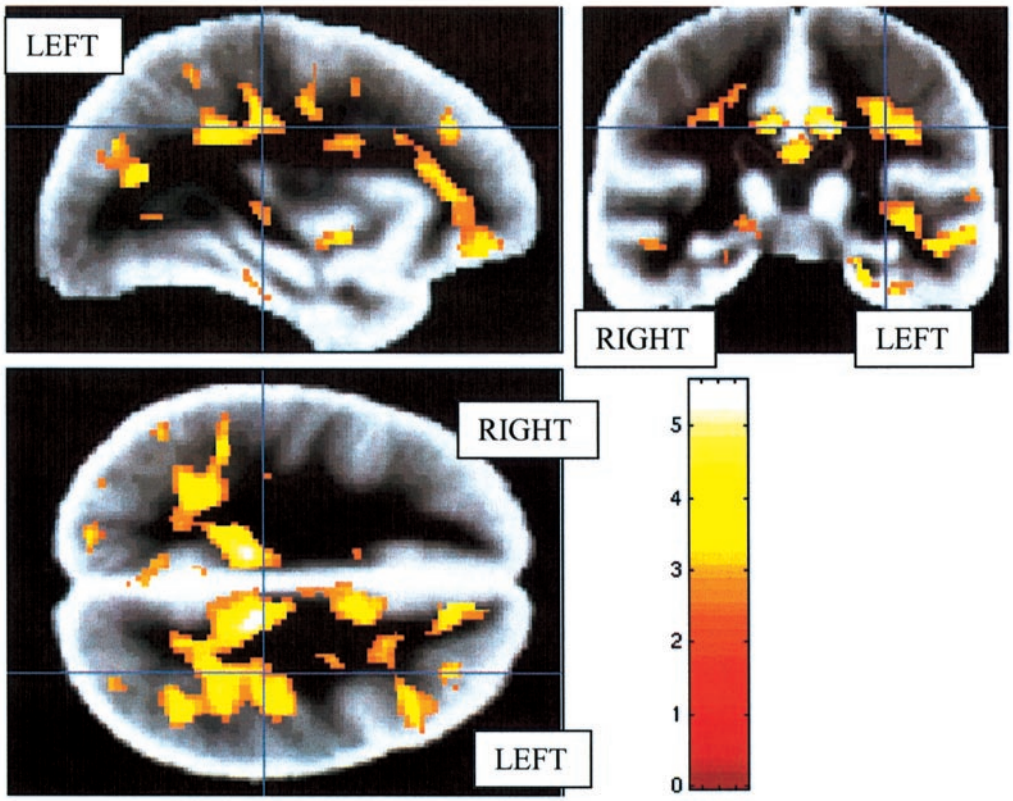

Figure 2. Age differences in the regional contrast ratio (rCR). Color-coded maps of the *t*-statistic for cross-sectional age effects on WM signal characteristics in the brain, measured by the rCR between WM and GM. To facilitate anatomical localization, significant voxels are displayed on a map of the average GM distribution.

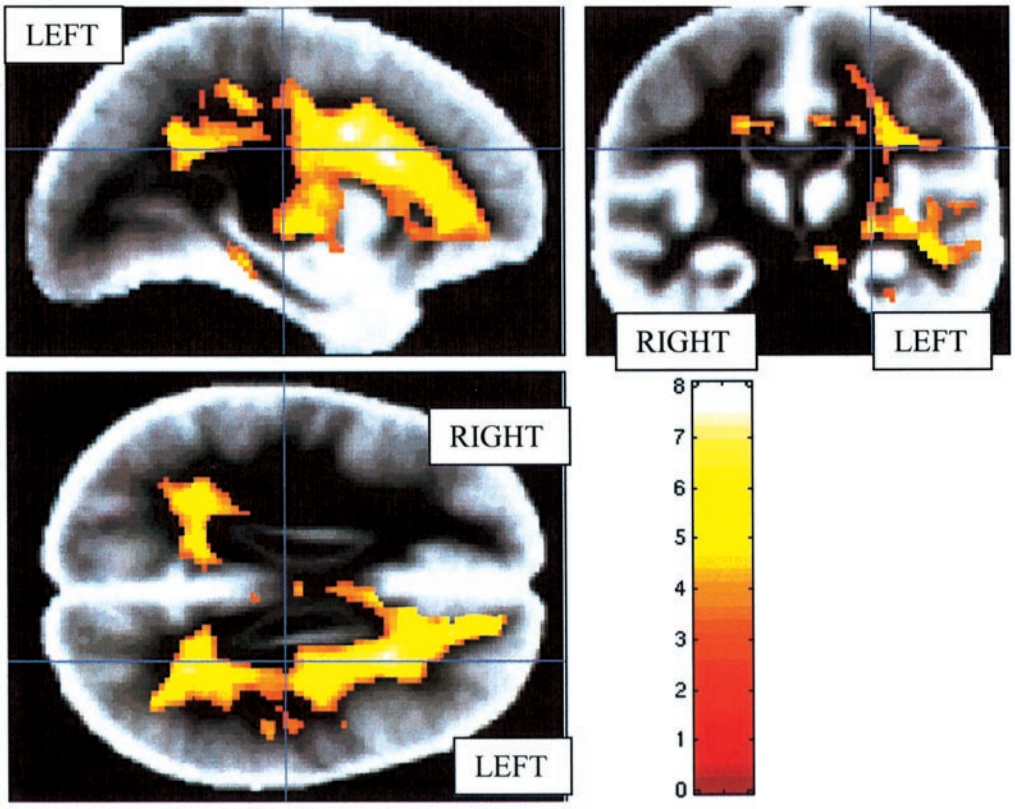

Figure 3. Longitudinal changes in regional contrast ratio (rCR). Color-coded maps of paired *t*-tests applied on the rCR images obtained over a 4 year interval. The left hemisphere displays significant longitudinal changes in frontal, parietal and temporal regions, while the right hemisphere displays significant changes only in a small area of the parietal WM.

Statistical parametric maps were also generated to test for sex differences in rCR. There were no significant sex differences in the spatial pattern of rCR at baseline. Moreover, no significant differences in the spatial distribution of longitudinal changes were found between men and women.

Discussion

Our results provide the first demonstration of longitudinal age changes in GM–WM tissue contrast and in regional WM signal intensities, the latter implying degenerative age changes in WM connectivity. Factors that may lead to signal changes include WM demyelination and changes in water, protein and mineral content of tissue. In fact, decreases in myelin and increases in water content of WM are known to occur in normal aging (Wiggins *et al.*, 1988) and age effects on T_1 relaxation times have been reported (Cho *et al.*, 1997). It is also possible that neuropathological abnormalities, such as deposition of amyloid plaques, may be reflected in signal changes in brain tissue. Our findings indicate that there are age-related changes in underlying tissue composition, but the cellular basis of these changes cannot be determined from standard magnetic resonance structural imaging protocols.

Our observations also demonstrate that degenerative age effects on WM connectivity are not uniform throughout the brain, but rather they have specific regional patterns. Most pronounced was the difference between left and right hemispheres, with the left hemisphere showing more rapid changes and larger age differences than the right hemisphere. This interhemispheric difference was pronounced primarily in frontal and temporal regions, and less pronounced in parietal association regions. Finally, occipital regions did not display any significant age differences or longitudinal changes, which is consistent with the relative preservation of functional activity in primary visual regions with aging (Murphy *et al.*, 1996). Our findings are complementary to recent studies using diffusion (Bozzao *et al.*, 2001; O'Sullivan *et al.*, 2001) and perfusion diffusion (Bozzao *et al.*, 2001) imaging, which have indicated changes in magnetic resonance signal characteristics with normal and abnormal aging. A complete characterization of such changes will most likely require a combined approach that examines all aspects of the magnetic resonance signal. One of the unique elements of our study is the use of high-dimensional spatial normalization transformations, which enabled a voxel-wise statistical analysis, rather than the coarser region-of-interest-based analysis.

An important finding of our study is the lack of associations between age changes in signal intensity and brain atrophy. This indicates that measures of tissue characteristics provide unique and complementary information to widely used morphometric measures. Measurements based on rWM-CR show stronger associations with age and can potentially be more sensitive than volumetric measures as indicators of preclinical disease, because they reflect changes in the underlying tissue composition. Volumetric changes are likely to occur later than signal changes, when loss of tissue causes displacement of well-identified features, such as tissue boundaries.

The extent to which subtle changes in periventricular regions contributed to local changes in these regions is unclear. It is important to note that our analysis was restricted to relatively healthy elderly subjects of the BLSA, who typically display only mild age-related periventricular signal abnormalities, often called 'hyperintensities' due to their bright appearance in T_2-weighted images. Any more extreme periventricular signal abnormalities did not affect our signal analysis, because these regions are typically classified as GM in T_1 images and were therefore excluded from the analysis that was restricted to WM points. The local analysis is, by definition, restricted locally, so any such signal abnormalities will affect only the voxels in which they appear. Misclassification of WM signal abnormalities as GM was also not likely to affect the global analysis, because these regions account for a very small percentage of the total WM volume. One goal of our continued follow-up studies is to characterize the progression of signal changes and to determine whether regions initially showing subtle changes are those that are more likely to contain 'hyperintensities' with advancing age.

In summary, our study is the first documentation of longitudinal age- and region-dependent changes in magnetic resonance signal characteristics of WM fibers, reflecting underlying degenerative effects of aging. Due to the limitations of structural magnetic resonance imaging, our study does not delineate the specific neurobiological processes underlying these changes. However, our findings highlight the potential utility of a novel approach to analysis of magnetic resonance images and suggest clear directions for more detailed *in vivo* imaging (e.g. magnetic resonance spectroscopy) and post-mortem neuropathological examinations. Continued longitudinal follow-ups of this sample will determine whether changes in tissue composition provide information useful in the preclinical identification of individuals vulnerable to memory problems and Alzheimer's disease.

Notes

This work was supported in part by contract NIH-AG-93-07 and by NIH grant R01-AG14971.

Address correspondence to Christos Davatzikos, Department of Radiology, JHOC 3230, Johns Hopkins University School of Medicine, 601 North Caroline Street, Baltimore, MD 21287, USA. Email: hristos@jhu.edu.

References

Ashburner J, Friston KJ (2000) Voxel-based morphometry: the methods. Neuroimage 11:805–821.

Benveniste H, Einstein G, Rim KR, Hulette C, Johnson GA (1999) Detection of neuritic plaques in Alzheimer's disease by magnetic resonance microscopy. Proc Natl Acad Sci USA 96:14074–14084.

Bookstein FL (1989) Principal warps: thin-plate splines and the decomposition of deformations. IEEE Trans Pattern Analysis Machine Intell 11:567–585.

Bozzao A, Floris R, Baviera ME, Apruzzese A, Simonetti G (2001) Diffusion and perfusion MR imaging in cases of Alzheimer's disease: correlations with cortical atrophy and lesion load. Am J Neuroradiol 22:1030–1036.

Cho S, Jones D, Reddick WE, *et al.* (1997) Establishing norms for age-related changes in proton T_1 of human brain tissue *in vivo*. Magn Reson Imaging 5:1133–1143.

Coffey CE, Wilkinson WE, Parashos IA, *et al.* (1992) Quantitative cerebral anatomy of the aging human brain: a cross-sectional study using magnetic resonance imaging. Neurology 42:527–536.

Collins DL, Zijdenbos AP, Baare WFC, Evans AC (1999) Animal + insect: improved cortical structure segmentation. In Proceedings of the Conference on Information Processing in Medical Imaging, IPMI '99. pp. 210–223.

Convit A, De Leon MJ, Tarshish C, *et al.* (1997) Specific hippocampal volume reductions in individuals at risk for Alzheimer's disease. Neurobiol Aging 18:131–138.

Davatzikos C (1997) Spatial transformation and registration of brain images using elastically deformable models. Comput Vis Image Understanding 66:207–222.

Davatzikos C (2000) Measuring biological shape using geometry-based shape transformations. Image Vis Comput 19:63–74.

Davatzikos C, Vaillant M, Resnick S, Prince JL, Letovsky SI, Bryan RN

(1996) A computerized method for morphological analysis of the corpus callosum. J Comput Assist Tomogr 20:88–97.
Freeborough PA, Fox NC (1998a) Modeling brain deformations in Alzheimer's disease by fluid registration of serial MR images. J Comput Assist Tomogr 22:838–843.
Freeborough PA, Fox NC (1998b) MR texture analysis applied to the diagnosis and tracking of Alzheimer's disease. IEEE Trans Med Imaging 17:475–479.
Gaser C, Volz HP, Kiebel S, Riehemann S, Sauer H (1999) Detecting structural changes in whole brain based on nonlinear deformations — application to schizophrenia research. Neuroimage 10:107–113.
Goldszal AF, Davatzikos C, Pham DL, Yan MXH, Bryan RN, Resnick SM (1998) An image processing protocol for qualitative and quantitative volumetric analysis of brain images. J Comput Assist Tomogr 22:827–837.
Jack CR Jr, Petersen RC, Xu Y, *et al*. (2000) Rates of hippocampal atrophy correlate with change in clinical status in aging and AD. Neurology 55:484–89.
Kaye JA, *et al*. (1997) Volume loss in the hippocampus and temporal lobe in healthy elderly persons destined to develop dementia. Neurology 48:1297–1304.
Kovalev VA, Kruggel F, Getz HJ, von Cramon DY (2001) Three-dimensional texture analysis of MRI brain datasets. IEEE Trans Med Imaging 20:424–433.
Miller MI, Christensen GE, Amit Y, Grenander U (1993) Mathematical textbook of deformable neuroanatomies. Proc Natl Acad Sci USA 90:11944–11948.
Mueller EA, Moore MM, Kerr CCR, *et al*. (1998) Brain volume preserved in healthy elderly through the eleventh decade. Neurology 51: 1555–1562.
Murphy DGM, DeCarli C, McIntosh AR, *et al*. (1996) Sex differences in human brain morphometry and metabolism: an *in vivo* quantitative magnetic resonance imaging and positron emission tomography study on the effect of aging. Arch Gen Psychiatry 53:585–594.
O'Sullivan M, Jones DK, Summers PE, Morris RG, Williams SCR, Markus HS (2001) Evidence for cortical disconnection as a mechanism of age-related cognitive decline. Neurology 57:632–638.
Pfefferbaum A, Mathalon DH, Sullivan EV, *et al*. (1994) A quantitative magnetic resonance imaging study of changes in brain morphology from infancy to late adulthood. Arch Neurol 51:874–887.
Pham DL, Prince JL (1999) Adaptive fuzzy segmentation of magnetic resonance images. IEEE Trans Med Imaging 18:737–752.
Pruessner JC, *et al*. (2000) Volumetry of hippocampus and amygdala with high resolution MRI and three-dimensional analysis software: minimizing the discrepancies between laboratories. Cereb Cortex 10:433–442.
Raz N, Gunning FM, Head D, *et al*. (1997) Selective aging of the human cerebral cortex observed *in vivo*: differential vulnerability of the prefrontal gray matter. Cereb Cortex 7:268–282.
Resnick SM, *et al*. (2000) One year changes in MRI brain volumes in older adults. Cereb Cortex 10:464–472.
Talairach J, Tournoux P (1988) Co-planar stereotaxic atlas of the human brain. Stuttgart: Thieme Verlag.
Thompson PM, MacDonald D, Mega MS, Holmes CJ, Evans AC, Toga AW (1997) Detection and mapping of abnormal brain structure with a probabilistic atlas of cortical surfaces. J Comput Assist Tomogr 21:567–581.
Wiggins RC, Gorman A, Rolsten C, *et al*. (1988) Effects of aging and alcohol on the biochemical composition of histologically normal human brain. Metab Brain Dis 3:67–80.
Yan MXH, Karp JS (1995) An adaptive Bayesian approach to three-dimensional MR image segmentation. In Proceedings of the XIVth Conference on Information Processing in Medical Imaging. pp. 201–213.